processes

MDPI

Article

Preparation and Characterization of *Lithraea molleoides* Gum Flour and Its Blend Films

Federico Becerra [1,*], Maria F. Garro [2,*], Gisela Melo [3] and Martin Masuelli [1,*]

[1] Instituto de Física Aplicada (INFAP-CONICET-UNSL)-Departamento de Química, Facultad de Química, Bioquímica y Farmacia, Universidad Nacional de San Luis, Ejército de los Andes 950, San Luis ZC 5700, Argentina
[2] Departamento de Farmacia, Facultad de Química, Bioquímica y Farmacia, Universidad Nacional de San Luis, Ejército de los Andes 950, San Luis ZC 5700, Argentina
[3] Facultad de Química, Bioquímica y Farmacia, IMIBIO-CONICET, Universidad Nacional de San Luis, Chacabuco 917, San Luis ZC 5700, Argentina
* Correspondence: federicobecerra456@gmail.com (F.B.); mfgarro@gmail.com (M.F.G.); masuelli@unsl.edu.ar (M.M.)

Abstract: *Lithraea molleoides* fruit gum (LMFG) is a valuable product obtained from the total hydrolysis of the fruit. The hydrolysis process involves three methods: thermal (LMFGT), alkaline (LMFGB), and acid (LMFGA). Through these methods, the aim is to break bonds and de-esterify polysaccharides, resulting in increased solubility and decreased molecular weight. The resulting hydrolysates are then combined with pectins in a 1:2 ratio to form films. In this study, the focus is on utilizing the hydrolysates of *Lithraea molleoides* gums for film applications, with an evaluation of their structural and physicochemical characteristics. The films produced exhibit excellent mechanical properties and low water vapor permeability, as well as exceptional thermal stability. These properties make them highly suitable for industrial films in pharmaceutical and food applications. This research highlights the potential of LMFG-based films as a viable solution for various industrial needs due to their outstanding performance across multiple parameters.

Keywords: *Lithraea molleoides* fruit gum; hydrolysis; films

Citation: Becerra, F.; Garro, M.F.; Melo, G.; Masuelli, M. Preparation and Characterization of *Lithraea molleoides* Gum Flour and Its Blend Films. *Processes* **2024**, *12*, 2506. https://doi.org/10.3390/pr12112506

Academic Editor: Clara Grosso

Received: 25 September 2024
Revised: 5 November 2024
Accepted: 6 November 2024
Published: 11 November 2024

1. Introduction

Packaging in the food industry uses synthetic plastics. The thermoplastics used for packaging—such as polystyrene, polyethylene, poly(ethylene terephthalate), and polypropylene—are disposable, generating waste, entering the environment, and undergoing degradation processes [1]. The disposal of nondegradable packaging waste of synthetic polymers is a global issue, and the scientific community is seeking to develop biodegradable packaging from renewable sources to reduce environmental impact [2]. Water-soluble gums are valuable in many fields, including adhesives, agriculture, biotechnology, ceramics, cosmetics, explosives, food, paper, textiles, and texturization, among many others [3–5]. Edible films and coatings, which are still used today, help prevent oxidative rancidity, preserve sensory qualities, maintain pigments, delay ripening, and extend the shelf life of various food products [6]. The proteins, polysaccharides, and their blends are used to make edible films/coatings containing antimicrobials, which have been demonstrated to be a useful tool as a stress factor to protect foodstuffs from spoilage flora and to decrease the risk of pathogen growth [7].

Carrageenan, cornstarch, and gelatin have been analyzed for their chemical, physical, and mechanical properties to explore how biodegradable alternatives from renewable sources can be used to produce films [8]. Starch formulations with a protein show potential because protein has characteristics that allow it to form a flexible film, not tear easily,

and rectify the physical characteristics of polysaccharide film [9]. Edible films and coatings enhance the quality of food products, protecting them from physical, chemical, and biological deterioration [10].

Regarding edible films and coatings with polysaccharides, proteins and lipids, exploring their sources, properties, and possible applications has the potential to substantially improve all of their properties [11]. In addition, improvements in the structural and barrier limitations of these films are required for better performance [12–14]. Coatings and films from polysaccharides, proteins, and lipids, with the addition of surfactants and plasticizers, are used for their barrier and mechanical properties which in turn depend on the film's formation process and composition. For edible coatings, the method of application to the product and the capacity of the coating to adhere to the surface are the most important parameters [15–18]. Recent research has covered advancements in edible films or coatings composed from natural plant compounds, highlighting their mechanical and physicochemical characteristics and the manner in which they promote sustainable practices in the packaging industry [19]. The importance of assessing the preformed matrix of edible films quantifies various parameters such as antimicrobial, mechanical, and optical properties since this envelope creates a modified atmosphere for straightening gas transfer (CO_2, O_2) and the aromatic compounds barrier [20].

The native or modified chitosans and chitooligosaccharides are associated with bioadhesive applications, adsorption, antimicrobial activities, and chelation in the wine industry [21]. There is potential for coatings based on xylan derivatives and chitosan to provide barrier properties and antimicrobial protection for packaging food [22]. One study has shown the functional properties of taro starch-reinforced polysaccharide-based films for active packaging, fabricating films containing chitosan, pullulan, and taro starch extracted from *Colocasia esculenta* (L.) Schott tubers using a wet-milling process [23]. *Gracilaria chouae* polysaccharide food packaging applied with carboxymethyl cellulose and lysozyme has also been studied [24].

Films derived from cellulose and its derivatives—including pectin, starch, alginate, chitosan, and pullulan—have been shown to reduce water vapor permeability [25]. Films produced from *Aloe vera* (L.) Burm. in β-hydroxy-β-methylbutyrate calcium and nanocellulose films have been shown to be effective for preserving the freshness of blueberries [26]. Polycaju and Tween have developed 80 edible coatings/films for protecting golden apples [27]. Propolis with cellulose, starch, chitosan, and alginate have been used for composite biodegradable active packaging [28]. Bionanocomposite films with plasticized whey protein isolate-jujube polysaccharide/starch nanocrystal blends have been studied in the context of packaging fresh-cut carrots [29]. A further study has considered the characterization of *Zizania latifolia* (Griseb.) Hance ex F. Muell. polysaccharide-corn starch composite films and their application in the post-harvest preservation of strawberries [30]. One study developed a polysaccharide-based composite film with antimicrobial properties to extend the shelf life of fresh-cut watermelon. Packaging tests demonstrated its potential for prolonging shelf life and showed excellent barrier and heat-sealing properties [31]. Xanthan gum/pullulan with grape seed extract (GSE) composite films have been shown to extend the shelf life of fresh-cut apples [32]. Soluble soybean polysaccharide and *Malva sylvestris* L. extract have been shown to extend food shelf life and detect shrimp spoilage [33]. *Auricularia auricula* (Bull.) J. Schröt. polysaccharide-based films have been shown to have an application in meat preservation [34]. Starch, chitosan, sodium alginate, and cellulose have been the subject of research focusing on improving the hydrophilic barrier and mechanical properties [35]. Carboxymethyl cellulose films have been enhanced with mulberry leaf polysaccharides [36]. Biodegradable, antimicrobial, and antioxidant packaging has been developed from chitosan, hyaluronic acid, and chondroitin sulfate [37]. Citric acid has been utilized to crosslink glycerol-plasticized soybean polysaccharide films, enhancing their water resistance, mechanical, UV-barrier, water vapor barrier, antioxidant, thermal, and antibacterial properties [38]. Renewable and biodegradable

fiber-based packaging materials are being developed to replace nonbiodegradable plastics. We created waterborne barrier coatings from natural polysaccharides, achieving a highly crosslinked polymer network that forms uniform, effective barrier layers on paperboard and molded pulp. These coatings offer excellent oil and grease resistance, reduced water sensitivity, and maintain recyclability [39–41].

Lithraea molleoides (Vell.) Engl. (Anacardiaceae) is a polygamous dioecious tree with persistent and dense foliage, also known as "molle de beber". It is distributed across northern and central Argentina, Bolivia, Brazil, and Uruguay. It is a tree that grows 3–8 m tall, with a globose crown, shiny leaves, and dark branches. The leaves are evergreen, alternate, shiny green, compound, with 3–5 lanceolate leaflets that come to a sharp point. The prominent secondary veins run parallel to each other. The small yellowish flowers are clustered in compound axillary racemes. The fruit is a globose drupe, with a greenish or white epicarp. It appears juicy when ripe, but is dry and breaks to release the seeds. It is 6–8 mm in diameter, whitish-green and shiny. It blooms from October to November and bears fruit from January onwards. These are edible; the indigenous Tehuelche people favored the fruits and also made chicha from the crushed seeds [42]. This paper concerns the fruit of LM, which has never been studied; nor have there been any publications on it.

In this study, *Lithraea molleoides* fruit gum (LMFG) was obtained from hydrolysis of the fruit. Three forms of hydrolysis were used: thermal (LMFGT), alkaline (LMFGB), and acid (LMFGA). The LMFG was analyzed by Proximate Analysis of Biomass, Antioxidant Activity Assays (Reducing Power, Hydroxyl Radical Scavenging, DPPH Scavenging Activity, Total Polyphenol Content), Fourier-Transform Infrared Spectroscopy, X-ray Diffraction (XRD), Differential Scanning Calorimetric Analysis (DSC), and Thermogravimetric Analysis. The aim of hydrolysis was bond breaking and de-esterification of polysaccharide, with the consequent increase in solubility and decrease in molecular weight. Blend films with pectins were prepared from LMFGTf (Thermal), alkaline LMFGBf, and acid LMFGAf gums. These films were characterized by Scanning Electron Microscopy–Electron Dispersive X-ray Spectroscopy (SEM-EDX), Mechanical Tests, Water Vapor Permeability and Biodegradability.

2. Materials and Methods

2.1. Raw Material

The *Lithraea molleoides* fruit, LMF, (voucher number: UNSL # 533 [42]) was collected in the countryside of San Francisco del Monte de Oro (32°36′00″ S, 66°07′30″ W) in San Luis, Argentina, in January 2022. The fruit was selected and washed with distilled water, placed in a polypropylene container, and dried at 60 °C for 24 h. All fruit (husk and seed) was ground and separated using 50 mesh, which generated LMF flour. All hydrolysis was performed at 80 °C for 6 h (thermal hydrolysis), at a concentration of 0.01 M NaOH (Anhedra, Argentina) for alkaline hydrolysis and HCl (Ciccarelli, Argentina) for acid hydrolysis. The soluble fraction was precipitated with ethanol/distilled water 70/30 and separated by filtration; the filtrate was concentrated at 60 °C for 8 h, and dried at 60 °C for 24 h. The nomenclature for the different flours was as follows: HLM for unhydrolyzed flour, LMFGT for thermal hydrolysis, LMFGB for alkaline hydrolysis, and LMFGA for acid hydrolysis [43]. The yield was calculated from 10 g of LMF, using the following equation:

$$Yield\% = 100\frac{LMF_{Hidr}}{LMF} \quad (1)$$

where LMF was the initial mass of the flour (10 g) and LMF_{Hidr} was the mass of resulting hydrolysate.

The synthesis of films was carried out by adding 2 g of pectin (MAC, Argentina) as a polymer matrix, 1 g of the different hydrolysates, and 1 mL of glycerin used as a plasticizer. The nomenclature for the different films that contained hydrolysates was as follows: LMFGTf for thermal hydrolysis, LMFGBf for alkaline hydrolysis, and LMFGAf for acid

hydrolysis. The pectin film (Pec2.5) was made by the casting method from 2.5 g of pectin (MAC, Argentina), then following the same procedure as the rest of the films.

2.2. Lithraea molleoides Fruit Gum Flour (LMFG)

2.2.1. Proximate Analysis of Biomass

In accordance with standard methods, the sample was macerated to a powder and subjected to proximate analysis (AOAC, 2012). The nitrogen content was determined using the Kjeldahl–Arnold–Gunning method, and total proteins were calculated using a factor of 6.25 (AOAC. 920.12). Protein productivity was also calculated and expressed as milligrams of protein produced per liter of culture per hour. Total fats were determined using the Soxhlet gravimetric method with petroleum ether (Sigma Aldrich, St. Louis, MA, USA) (AOAC 945.39), while crude fiber was determined using the digesting sample method with H_2SO_4 and NaOH (Sigma Aldrich) (AOAC 962.09). Ashes were determined using the weight difference method after calcining the sample (AOAC 945.46), and moisture content was determined through heating under reduced pressure (AOAC 945.46). Carbohydrates were indirectly calculated as follows: Total carbohydrates = 100 − (Proteins + Total Fat + Moisture + Ash). Following these established methods ensured accuracy and consistency in our analysis, providing valuable information for further research or application within various industries [44].

2.2.2. Antioxidant Activity Assays

Reactive oxygen species (ROS) are known to cause liver-damaging oxidation and loss of bodily functions. Among these ROS, superoxide anion radicals ($O_2^{\bullet-}$) and DPPH radicals are particularly detrimental to the body. Therefore, the determination of these ROS is crucial in the study of novel polysaccharides. Understanding the impact of ROS on the body's functions is essential for developing effective treatments for liver damage and oxidative stress-related conditions. By studying how novel polysaccharides interact with and potentially neutralize these harmful free radicals, researchers can advance our understanding of their potential therapeutic benefits. Investigating the effect of novel polysaccharides on reactive oxygen species could lead to breakthroughs in medical treatment and preventive care. The determination of ROS is a key step in this research process, laying the groundwork for potential advancements in healthcare and wellness [45]. The role that reactive oxygen species play in liver damage underscores the importance of studying novel polysaccharides as potential countermeasures. The determination of these harmful free radicals serves as a critical starting point for further advancements in medical research and treatment options.

Reducing Power

The reducing power assay, as described by reference [45], involved several steps to determine the reducing power of polysaccharide solutions. This method required precise measurements and careful incubation to ensure accurate results. The addition of reagents such as phosphate buffer (2 M, pH 6.6), potassium ferricyanide (1% *w*/*v*), trichloroacetic acid (2.5 mL 10% *w*/*v*), and ferric chloride (0.2 mL) were crucial in stopping the reaction and measuring the absorbance at 700 nm. The procedure was conducted in triplicate to ensure reliability, with gallic acid serving as a positive control for comparison. The results were expressed as μeq/mL of gallic acid. This meticulous approach allowed for a thorough assessment of the reducing power of polysaccharide solutions, demonstrating the importance of precision in scientific methodologies.

DPPH Scavenging Activity

DPPH radical scavenging activity was assessed using a method described by reference [45] with some adjustments. The process involved adding 0.5 mL of polysaccharide solution (0.1–1 mL) to a 90% ethanolic solution of DPPH (0.15 M) and incubating it in

darkness for 30 min before measuring absorbance at 517 nm. The total antioxidant content was calculated as a percentage of antioxidant activity (% AA) using the equation:

$$AA(\%) = \frac{(Ac-(Am-Ab))}{Ac} \times 100 \quad (2)$$

where A_c is the absorbance of the control, A_m is the sample absorbance, and A_b is the blank absorbance. The procedure was conducted in triplicate, and ascorbic acid was used as a positive control. A calibration curve for ascorbic acid was also prepared and measured to express the results in mg/mL equivalents of ascorbic acid. These meticulous measurements and calculations provided valuable insights into the antioxidant properties of polysaccharides, contributing to our understanding of their potential health benefits.

2.2.3. Total Polyphenol Content

The determination of total phenolic compounds was conducted in accordance with the Folin–Ciocalteu method [46,47], with some modifications to ensure accuracy and precision. A 5 mL aliquot of the sample was carefully measured and combined with 1.5 mL of Folin–Ciocalteu reagent (2 N) and 15 mL of Na_2CO_3 solution (15%) in a volumetric flask, resulting in a final volume of 25 mL that was completed with distilled water. The resulting mixture was allowed to stand in a location shielded from light, at room temperature for a duration of 2 h to facilitate the reaction. Following completion of the reaction, the absorbance was measured at 760 nm using appropriate instrumentation. In order to establish calibration curves and ensure accuracy, six concentrations ranging from 1 to 6 mg/L were prepared using gallic acid (GA) as a reference standard. To validate results, this entire procedure was meticulously performed twice in order to confirm reproducibility and reliability.

2.2.4. Fourier-Transform Infrared Spectroscopy

In the field of analytical chemistry, Fourier-transform infrared (FTIR) spectroscopy is a widely used technique for identifying and analyzing chemical compounds. In this study, FTIR spectra were obtained using two different modes—diffuse reflectance (DRIFTS) and transmission—with the use of a Nicolet PROTEGE 460 Spectrometer, USA. The operational range for the spectra collection was set from 700 to 400 cm^{-1}, allowing for comprehensive analysis of the samples. Furthermore, each sample was scanned 64 times to ensure accuracy and reliability in the results. The choice to use both DRIFTS and transmission modes provided valuable insight into the chemical composition and structure of the samples under investigation. This comprehensive approach allowed for a thorough understanding of the molecular vibrations present in the samples across a wide range of wavelengths. Overall, this study showcases meticulous attention to detail in experimental design and execution, aiming to provide high-quality data for further analysis and interpretation. The use of advanced instrumentation coupled with precise scanning parameters ensures that the FTIR spectra obtained are robust and reliable, laying a solid foundation for meaningful insights into the chemical nature of the samples [48].

2.2.5. X-ray Diffraction (XRD)

X-ray diffraction (XRD) studies were conducted utilizing state-of-the-art Rigaku equipment, specifically the model ULTIMA IV type II, manufactured in Tokyo, Japan. This equipment was equipped with a Cu Kα lamp with a wavelength (λ_B) of 1.54 Å and a nickel filter to ensure accurate and precise measurements. The operational range for the 2θ angle was set from 3° to 60°, with the instrument being operated at 30 kV and 20 mA. A sweep rate of 3° per minute with a reading step of 0.02° was utilized in continuous mode to ensure comprehensive data collection. The $d_{spacing}$, or average intercatenary distance, was determined by applying Bragg's equation:

$$d_{spacing} = \frac{n\,\lambda_B}{2sin\theta_B} \quad (3)$$

where $d_{spacing}$ represents the intercatenary distance, n is an integer value determined through analysis, λ_B denotes the X-ray wavelength used, and θ_B refers to Bragg's angle [48].

$$I_{cr} = 100\ \frac{I_{max} - I_{ad}}{I_{max}} \quad (4)$$

Moreover, the crystalline index (I_{Cr}) was calculated from the normalized diffractogram using peak intensities at lattice plane reflection indices such as 110 lattices (I_{max}), which is observed at an angle of approximately 21° corresponding to maximum intensity. Additionally, amorphous diffraction data I_{ad} at an angle of approximately 15° was utilized in determining I_{Cr} following methods outlined in previous literature [49,50].

2.2.6. Differential Scanning Calorimetric Analysis (DSC)

Differential scanning calorimetry (DSC) was conducted using the STA 449F3-Jupiter equipment manufactured by Selb, Germany. To begin the analysis, approximately 5 mg of the biopolymer sample was carefully placed in an alumina crucible. The sample was then subjected to a controlled heating process, starting from an initial temperature of 25 °C and steadily increasing to a maximum temperature of 400 °C. This heating process was carried out at a constant rate of 5 °C per minute under a dynamic nitrogen atmosphere with a flow rate set at 25 mL per minute [51]. These specific parameters were chosen in order to accurately measure and analyze the thermal behavior and properties of the biopolymer sample, allowing for precise determination of its characteristic transitions and thermal stability under these controlled conditions.

2.2.7. Thermogravimetric Analysis

The thermal stability of the polysaccharide films was assessed through a comprehensive thermogravimetric analysis (TGA). The TGA determinations were carried out utilizing a TG 295 analyzer from TA Instruments, Inc., located in New Castle, DE, USA. The analytical conditions included a heating rate of 10 °C/min in a N_2 (99.99%) atmosphere with a flow rate of 50 mL/min, which had been pre-filtered. Moreover, the temperature axes for thermogravimetric analysis were calibrated using indium (99.99%, with a melting point of 156.60 °C) and the Curie point of Ni (353 °C). Empty aluminum pans (40 mL) were utilized as reference materials and polysaccharide samples weighing approximately 8 mg were employed [51].

2.3. Lithraea molleoides Fruit Gum Films (LMFGf)

2.3.1. Scanning Electron Microscopy–Electron Dispersive X-ray Spectroscopy (SEM-EDX)

The film's morphology was meticulously analyzed using a state-of-the-art scanning electron microscope, the LEO 145VP, from a manufacturer located in Los Altos, CA, USA. Additionally, the energy dispersion X-ray analysis was conducted using the highly advanced EDS Genesis 200 by EDAX, also based in Los Altos, CA, USA. Prior to surface analysis with SEM, the samples underwent a preparation process involving immersion in liquid nitrogen and subsequent coating with gold. The observations of biopolymer samples were carried out under high vacuum conditions, and the resulting EDAX spectrums were obtained with an acceleration voltage of 120 kV [51], ensuring precise and accurate data collection for thorough investigation.

2.3.2. Mechanical Tests

The mechanical properties of the materials were assessed using a Brookfield CT3 instrument from the USA, in accordance with the ASTM D882 requirements, at a consistent

traction speed of 0.1 mm/min. The experimental procedure for determining these properties was conducted at a temperature of 25 °C and relative humidity of 40%, with each test performed in triplicate. Test samples measuring 40 mm in length by 10 mm wide were utilized, with thickness measurements taken for each film using a micrometer. Data on force (F) and deformation (Δl) were collected until the breaking point was reached. Tensile strength (σ) was calculated by dividing the maximum load by the specimen's initial cross-sectional area (A). Percentage elongation at break (% ε) was determined as a percentage change from the specimen's initial length (l = 40 mm) at failure. Lastly, elastic modulus, or Young's modulus (E), was derived from the slope of the stress (σ) vs strain (ε) curve in the elastic region, which represents the linear part of the curve [51,52].

$$E = \frac{\sigma}{\varepsilon} \tag{5}$$

$$\sigma = \frac{F}{A} \tag{6}$$

$$\varepsilon = \frac{\Delta l}{l_0} \tag{7}$$

2.3.3. Water Vapor Permeability

The determination of water permeability was carried out using equipment from Electrotech Systems, Chicago, IL, USA, in which temperature and humidity measurements are measured and controlled by sensors located in a closed system. The weight change was obtained by a RADWAG balance (Radom, Poland) with a precision of 0.1 mg, and a Kolfe thickness micrometer (Munchen, Germany), with accuracy of 0.1 mg. The film samples, 25 mm in diameter, were cut, and their thicknesses were measured. They were then placed in the perforated caps of bottles containing 20 g of silica gel. Each bottle with silica gel was weighed, and, once sealed with the corresponding cap, the experiment began. The bottles were placed in equipment maintained at 30 °C and 85% relative humidity. During the first hour, the samples were weighed every five minutes. From the second to the third hour, measurements were taken every fifteen minutes. Afterward, the samples were weighed at one-hour intervals until a total period of 24 h was reached (ASTM E96). The permeability mechanism can be described for a homogeneous polymer film of thickness under a permeant pressure difference p (with p1 > p2) and permeant concentrations c across the film (with c1 > c2).

$$\tau = \frac{Q}{t\,A} \tag{8}$$

$$P = \frac{\lambda}{\Delta P}\,\tau \tag{9}$$

where τ is transmission speed (ng/m²s), t is measurement time(s), λ is thickness of film (m), Q is permeating mass (ng), A is area of cell (m²), and ΔP is pure water vapor pressure (4238.605 Pa) [51–53].

2.3.4. Biodegradability

The process of biodegradation is a complex and crucial aspect of the life cycle of biopolymers. It involves the breakdown and transformation of these materials through the enzymatic action of microorganisms such as bacteria, yeasts, and fungi. This process can result in total or partial degradation, with partial degradation leading to changes in chemical composition and loss of specific properties. The complete degradation of a material occurs when it is entirely consumed by microorganisms, resulting in the production of methane or CO_2 depending on the conditions. In a recent study, a covered container was filled with moistened soil samples at 85% relative humidity, and samples were monitored over a 120-day period under mesophilic conditions at 30 °C to assess biodegradation rates

[52–54]. The findings from this study shed light on the intricate mechanisms involved in biodegradation processes and their potential implications for sustainable waste management practices.

3. Results

3.1. Lithraea Molleoides Fruit Gum Flour (LMFG Flour)

3.1.1. Proximate Analysis of Biomass and Antioxidant Capacity

The percentage yield of the gum obtained was calculated from 10 g of dried fruit, where R_e% is the ratio of what was obtained and the sample. The yield was determined after filtration of the solution and the soluble filtrate was precipitated with ethanol/water in a 70/30 ratio. No information is provided about the type and structure of the polysaccharide obtained, which will be studied in future publications. The yield for the LMFGB flour was 33.88%, 15.43% for the LMFGA, and 11.11% for the LMFGT. This means that alkaline hydrolysis was more efficient in extracting polysaccharide, while thermal hydrolysis was less efficient. Taking into account the fiber analysis, a similar but numerically greater trend can be seen; this is because the technique performs total hydrolysis, with the amount of sample being much higher than the yield. The amount of protein was tiny and less than 0.1%. Ashes gave mixed results, but the interesting fact is that untreated flour (HLM) was similar to thermal flour, repeating the pattern in total fats. As for total fats, these were partially eliminated during alkaline or acid hydrolysis in a similar way. Moisture was similar to all flours except HLM. For proximate analysis of biomass, see Table 1.

Table 1. Proximate analysis of biomass.

	Moisture (%wt.)	Ash (%wt.)	Total Fats (%wt.)	Proteins (%wt.)	Fibers (%wt.)
HLM	10.60 ± 0.25	1.84 ± 0.02	9.92 ± 0.33	0.0454	15.22 ± 0.53
LMFGT	2.40 ± 0.74	1.45 ± 0.03	7.30 ± 0.31	0.0851	28.49 ± 1.24
LMFGA	3.12 ± 0.18	0.82 ± 0.01	3.40 ± 0.14	0.0189	27.78 ± 1.55
LMFGB	3.25 ± 0.17	0.84 ± 0.01	2.84 ± 0.13	0.0330	42.20 ± 1.89

However, not all polysaccharides exhibit high antioxidant activity, as is the case with LMFGT, LMFGA, and LMFGB. Some studies have shown that certain types of polysaccharides have limited antioxidant activity [55], meaning that their ability to protect cells from oxidative stress is lower compared to other compounds (see Table 2). This limited antioxidant activity may be due to several factors. First, the chemical structure of a polysaccharide can influence its ability to act as an antioxidant agent. For example, some polysaccharides may have side chains or functional groups that make it difficult for them to interact with free radicals. Furthermore, the degree of branching and the chain length of the polysaccharide can also affect its antioxidant activity. Longer polymers tend to have a greater ability to trap and neutralize free radicals due to the greater molecular surface available to interact with them. On the other hand, external factors such as hydrolysis processing can also decrease the antioxidant activity of polysaccharides. During these processes, adverse conditions such as high temperatures or exposure to oxygen can cause modifications in the chemical structure of the compound, reducing its effectiveness as a protective agent against oxidative stress. In summary, although polysaccharides are known for their various biological and nutritional benefits, not all of them have high antioxidant activity. It is important to take these aspects into account when choosing natural or supplemental sources of polysaccharides for therapeutic purposes.

Table 2. Antioxidant activity of the different gums obtained.

	Reducing Power (μeq GA/mL)	DPPH Scavenging Activity (μeq AA/mL)	Total Polyphenols (μeq GA/mL)
HLM	4.04 ± 0.22	14.78 ± 0.55	13.13 ± 0.39
LMFGT	1.91 ± 0.17	3.48 ± 0.22	28.58 ± 0.62
LMFGA	3.49 ± 0.33	2.71 ± 0.37	11.96 ± 0.48

LMFGB	9.91 ± 0.42	9.46 ± 0.45	41.82 ± 1.06

3.1.2. XRD

Amorphous polysaccharides are an essential component of many natural and synthetic materials. Understanding their structural properties is crucial for various fields, including pharmaceuticals, food science, and material engineering. One method of analyzing these polysaccharides is through X-ray diffraction (XRD) data. The XRD data of amorphous polysaccharides provide valuable insights into their molecular arrangement. In this particular case (Figure 1), the 2θ values for LMFGT, LMFGA, and LMFGB are 20.18, 20.62, and 20.34, respectively. Additionally, the $d_{spacing}$ values for LMFGT, LMFGA, and LMFGB are recorded as 4.39 nm, 4.30 nm, and 4.36 nm respectively (see Table 3). These numerical values serve as a foundation for further analysis of the amorphous polysaccharides' structure and characteristics, and comparing the different peaks in the X-ray diffraction pattern with standard references or known structures of similar compounds or polymers can provide valuable information about the arrangement at atomic level.

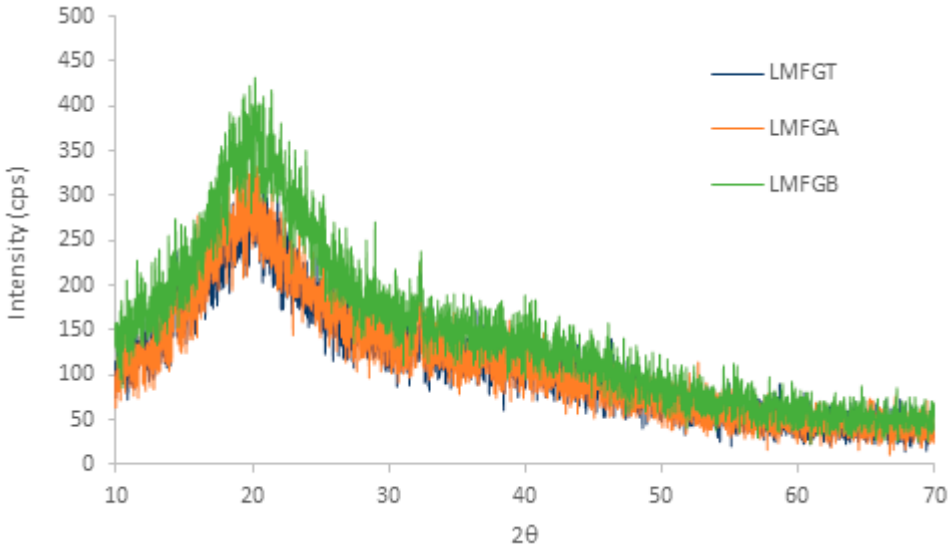

Figure 1. XRD of gums.

Table 3. XRD data of gums.

Flour	2θ	$d_{spacing}$ (nm)	I_{Cr} %
LMFGT	20.18 ± 0.81	4.39 ± 1.03	47.75 ± 1.23
LMFGA	20.62 ± 0.79	4.30 ± 0.98	48.10 ± 1.01
LMFGB	20.34 ± 0.84	4.36 ± 0.95	48.83 ± 0.98

These data can be used to deduce important information about these amorphous polysaccharides, such as intermolecular distances between chains or structural modifications due to environmental changes like moisture content or temperature fluctuations. Furthermore, these findings could help in developing new materials with enhanced functionalities by modulating their structure at molecular level, hence improving applications in the packaging industry to achieve better barrier properties against gases like oxygen, which will improve the shelf life of food products in contact with it. The I_{Cr} data are lower compared to those obtained by chitosan and its performance in an active film with quercetin and *Phaseolus polyanthus* Geenm. starch [55]. Similar results have been observed in chitosan, with 2θ of 20.07 corresponding to the crystallographic planes (110) with I_{Cr} of 40–42% [56]. In reference [57], the objective was to determine the physicochemical characteristics of Sac-Beh corn starch and *Delonix regia* (Boj. ex Hook.) Raf. galactomannan and use

them to produce films with vanillin; the results showed potential use of an edible film material for preservation of climacteric fruits, with crystallographic data similar to this paper. The properties of galactomanan bioplastics from *Prosopis juliflora* with citric acid is a similar case [58]. In this paper, the crystallinity index indicates that the different hydrolysates are amorphous.

3.1.3. FTIR

The infrared spectrum in Figure 2 shows several prominent absorption bands. The –OH stretching is observed at 339 cm^{-1}, indicating the presence of hydroxyl groups. The C–H band is located at 2927 cm^{-1}, and the carbonyl band is seen at 1743 cm^{-1}. Furthermore, the carboxylate group displays a distinct carbonyl band at 1621 cm^{-1} (C=O from $–COO^-$). The C−H side-chain bending $–CH_2OH$ exhibits multiple bands at 1413 cm^{-1}, 1375 cm^{-1}, and 1327 cm^{-1}. Additionally, a strong absorption peak is observed at 1242 cm^{-1}, corresponding to C−O−C stretching. Furthermore, the absorption peaks in the range of 1074 cm^{-1} to 1047 cm^{-1} are assigned to C−O glucopiranosic bending. Lastly, signals for out-of-plane bending C−O are noted at the frequencies of 781–777 and 704 cm^{-1} [55–59]. This comprehensive analysis provides valuable insight into the molecular structure and composition of the compound under investigation.

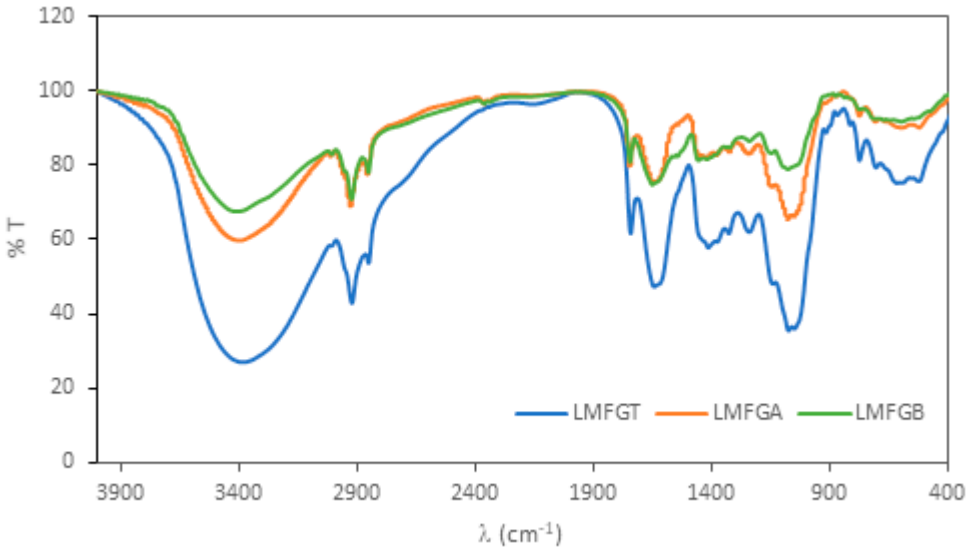

Figure 2. FTIR of gums.

3.1.4. DSC

Glass transition temperature (T_g) is a critical property of polymeric materials, as it marks the onset of significant molecular motion and can have a profound effect on the material's mechanical and thermal properties. In the case of three particular films, as shown in Figure 3, it was found that the T_g fell within a range of 40 to 50 °C. This broad range highlights the difficulty in pinpointing an exact T_g for these films, as it is not a sharply defined transition. On the other hand, the melting temperatures (T_m) are more readily observable and were determined to be 134 °C for LMFGT, 143 °C for LMFGA, and 132 °C for LMFGB. The relatively close proximity of T_m values for LMFGT and LMFGB indicates similarities in their molecular structures and bonding interactions. However, the higher Tm value for LMFGA suggests that its molecular structure possesses stronger intracatenary hydrogen bonding. This difference in melting temperatures can be attributed to variations in molecular packing arrangements within the films.

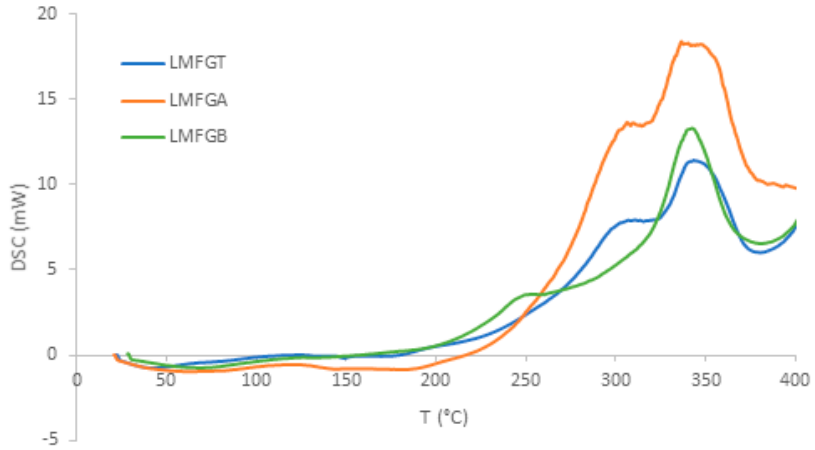

Figure 3. DSC of gums.

The stronger intermolecular interactions present in LMFGA result in a higher energy barrier required to disrupt these bonds and initiate melting. Understanding these thermal properties is crucial for predicting how these films will behave under different processing conditions or when subjected to varying environmental factors such as temperature changes. By elucidating how molecular structure influences thermal behavior, researchers can better tailor these materials for specific applications. The glass transition temperature may prove elusive due to its diffuse nature, but melting temperatures offer insight into the differences in molecular packing and strength, as, for example, in the case of carrageenan 2%/PVA8% films with T_g of 217.57 °C [59]. According to reference [60], the T_g of pectin is 70.8 °C and the T_m is 119.5 °C. This explains that the 1:2 ratio of pectin and LMFG at different hydrolysis is predominant over pectin, mainly due to the presence of LMFG.

In studying the intrinsic viscosity and molecular weight data (see reference [43]) it becomes evident that alkaline hydrolysis is the most energetically favorable process. This conclusion is drawn from the decrease in these parameters compared to thermal and acid hydrolysis. The nature of the biopolymer, a polysaccharide rich in hydroxyl and carboxyl groups, plays a significant role in this phenomenon. The incorporation of Na^+ by the carboxyl group increases solubility and promotes greater bond breaking during alkaline hydrolysis. Conversely, acid hydrolysis leads to greater unwinding of the polysaccharide, resulting in increased solubilization of groups and subsequent higher values for hydrodynamic radius and hydration value. These findings shed light on the intricate behavior of biopolymers under different hydrolytic conditions.

3.1.5. TGA

The thermal stability of LMFGT, LMFGA, and LMFGB has been determined to be 184.7 °C, 200 °C, and 186.4 °C, respectively [59]. This data confirms the effect of intrachain hydrogen bonds on the thermal stability of these films, with LMFGA exhibiting the highest stability due to the presence of these bonds (see Figure 4). These findings are significant in understanding the properties and potential applications of these materials in various industries. The identification of specific factors contributing to thermal stability will aid in further research and development efforts aimed at enhancing the performance of these films for practical use. The thermal stability of pectins is up to 215 °C [60]; although this is greater than those with LMFG, this may be due to the fact that they have fewer functional groups that can be oxidized.

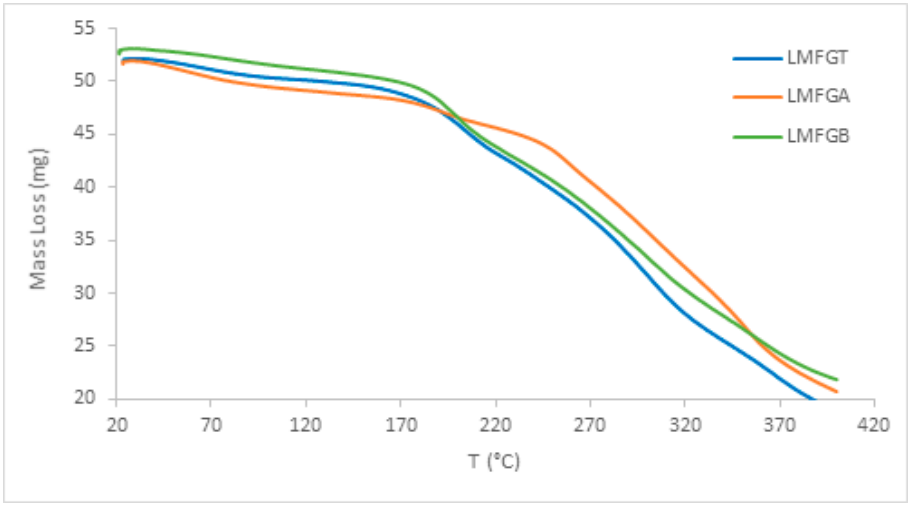

Figure 4. TGA of gums.

3.2. Lithraea molleoides Fruit Gum Films (LMFG Films)

3.2.1. SEM-EDX

The surface images show a slight undulation of a type resembling low mountains and shallow valleys. There are also certain isolated particles that are cellulosic remains that do not affect permeability. The surface image (Figure 5) in LMFGTf is smooth, while the undulations are more marked in the LMFGBf surface image. Regarding the presence of sodium on the surface of the films, this follows the sequence LMFGBf > LMFGTf > LMFGAf. The presence of sodium accounts for an increase in the rigidity of the film due to the presence of –COONa, a phenomenon evidenced in the mechanical tests, discussed later [56]. The pectin films appear homogeneous on the surface except for some particles and imperfections in minor quantities and a morphology similar to craters, valleys, and peaks (not acute) [60].

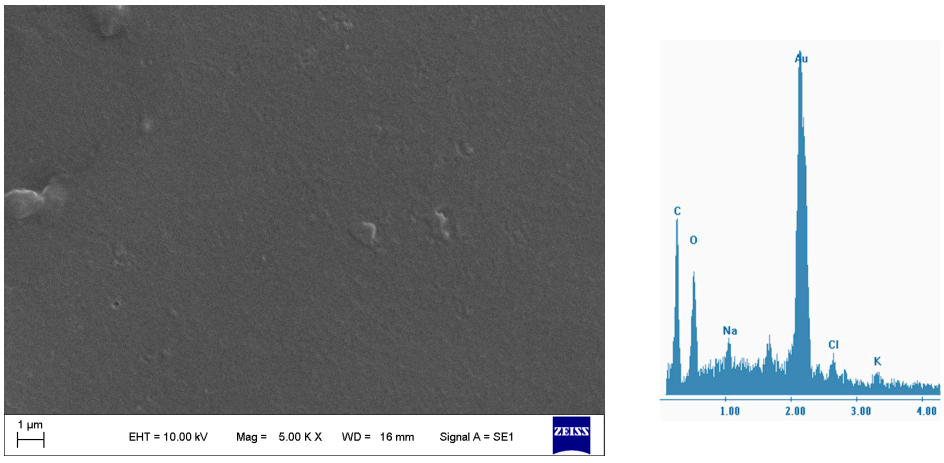

(**a**)

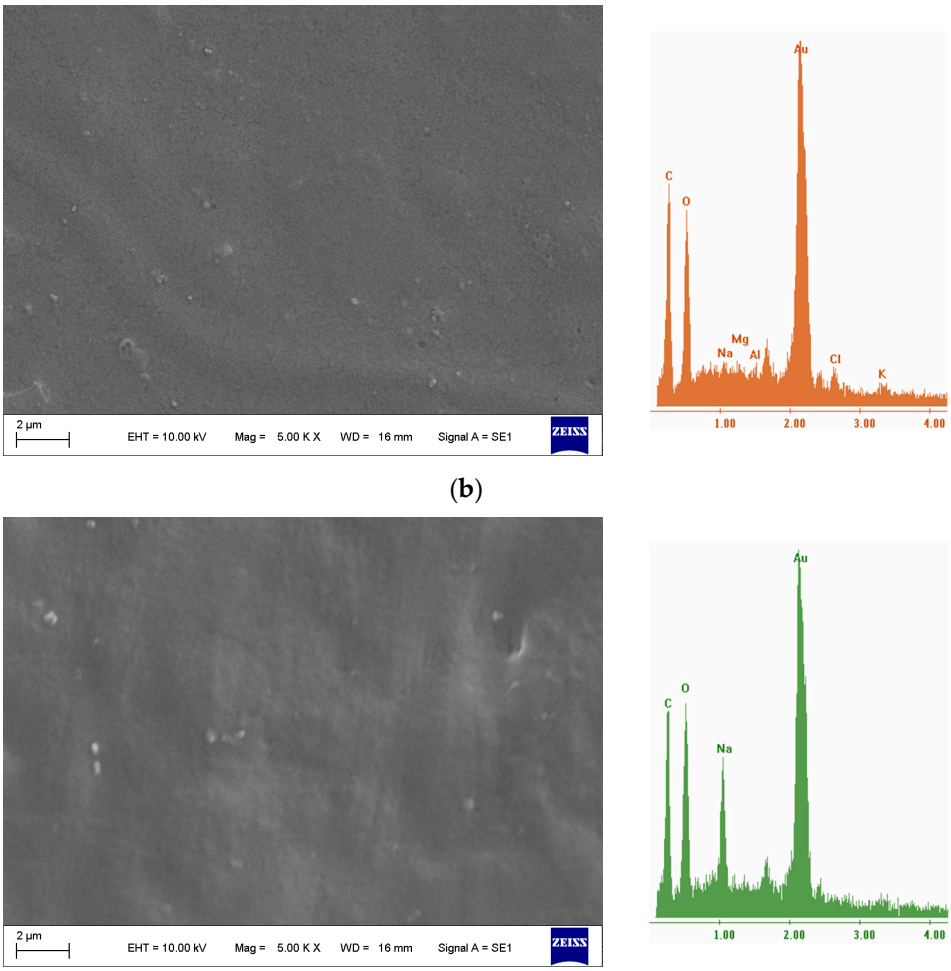

Figure 5. SEM surface images of (**a**) LMFGTf, (**b**) LMFGAf, and (**c**) LMFGBf, each with its corresponding elemental analysis by EDX.

In Table 4, the semi-quantitative analyses of the membranes under study can be observed, highlighting the presence of Na, Cl, and K in the LMFGTf and LMFGAf membranes. In LMFGAf, Na is scarce, because it is removed by the presence of HCl. While LMFGBf presents a large amount of Na, this does not affect the mechanical and permeability properties, as will be seen later.

Table 4. SEM-EDX semi-qualitative analysis.

	LMFGTf	LMFGAf	LMFGBf
C%	54.98	41.96	40.88
O%	34.84	38.18	43.91
Na%	4.03	0.80	30.68
Cl%	3.03	6.42	-
K%	3.11	5.20	-

3.2.2. Mechanical Test, WVP-Water Vapor Sorption (WVS)

Water vapor transport from the atmosphere through the packaging to the product is assessed by the WVP, see Figure 5. High or low water vapor permeability of packaging is prescribed for fresh or dehydrated vegetable products, in this case from 0.97 to 2.06 ng.m/m^2 s Pa. However, highly water permeable materials may have limited use as food packaging, as Pec2.5 with 0.55 ng.m/m^2 s Pa, because undesirable reactions promoted by

water and the carbohydrates, lipids, and proteins in the food may occur, decreasing its shelf life [26,53,54].

WVP in films with glycerol at 25 °C of pectins (without glycerol) is 1.6–4.7, chitosan 2% is 4.8–7.3, starch/chitosan is 0.15–3.3, sago starch/alginate is 20.7–34.6, cassava starch 5% is 54–139, gellan 0.5% is 18–23, and alginate 1.5% is 7–14 [7]. The units of WVP used here are similar to those used in this paper, according to reference [7]. In the case of aloe vera in β-hydroxy-β-methylbutyrate calcium and nanocellulose films [26], these have a lower WVP compared to those made in this paper; this is because these films have a greater affinity for water due to the greater amount of hydrogen bonds. The same can be observed in pectin/chitosan films with noni fruit extract, where values range from 1.1 to 2.3 ng m/m^2 Pa s [61].

Mechanical tests account for the physical integrity of the material under study, including its stability when a force is applied to it. The films had dissimilar responses to the applied force: for example, in Table 5, LMFGTf and LMFGBf have a low maximum stress at break and a similar maximum elongation at break between 19–25%, with a Young's modulus of 19–26 MPa. The LMFGAf film has a similar maximum elongation at break of 25.58%, σ_{max} of 21.87 MPa with an E of 47.23 MPa; that is to say, the film is more rigid, perhaps because its high molecular weight of 589,000 g/mol causes this response in the film. For thermal and alkaline hydrolysis, the fruit of *Lithraea molleoides* responds in a similar way, which causes the pectin polymer matrix to have a similar response and does not show synergism. However, acid hydrolysis compromises the polymer matrix, improving the rigidity of the material; this is due to a greater interaction between the pectin polymer matrix and LMFGAf through an improvement in hydrogen bond interactions. Another factor to take into account is the thickness of the film, which shows different mechanical properties due to the greater force to be applied. The mechanical tests in this case are practically similar to those observed below. As for the mechanical test data of Pec2.5, ε_{max} is 20.08%, σ_{max} is 23.8 MPa, and E is 32.85 MPa. These data for pure pectin are similar to those for LMFAf, where the interactions are not very marked, which means they are structurally and chemically similar. As for the mechanical tests in reference [7], the ε_{max} for pectins (without glycerol) was 0.8–1.2, chitosan 2% was 18–106, starch/chitosan was 61–152, sago starch/alginate was 3.7–13.2, cassava starch 5% was 39–164, and alginate 1.5% was between 5 and 20. While σ_{max} (MPa) for pectins (without glycerol) was 13–25, chitosan 2% was 5.5–21.3, starch/chitosan was 61–152, sago starch/alginate was 13–16, cassava starch 5% was 1–4.7, and alginate 1.5% was 23–160 [7].

Table 5. Mechanical properties and water vapor permeation of gums (e is thickness).

Films	e (μm)	ε_{max}%	σ_{max} (MPa)	E (MPa)	WVP P (ng.m/m^2 s Pa)
Pec2.5	207.8 ± 9.2	20.08 ± 0.90	23.79 ± 0.97	32.85 ± 1.1	0.55
LMFGTf	224.4 ± 8.1	24.47 ± 0.78	8.44 ± 0.34	19.65 ± 0.91	0.97
LMFGAf	264.6 ± 6.5	25.58 ± 0.06	21.87 ± 0.87	47.23 ± 0.82	1.52
LMFGBf	221.9 ± 5.8	19.40 ± 0.88	13.37 ± 0.56	26.05 ± 0.89	2.06

3.2.3. Biodegradability

The biodegradability of the films under study indicates a rapid decomposition process, with almost total breakdown occurring around 10 days and Pec2.5 in 7 days. The LMFGTf was 9.7 d, LMFGAf was 9.9 d, and LMFGBf was 10.1 d. This phenomenon is attributed to the consumption of these polysaccharide materials by microorganisms at a temperature of 30 °C and with a relative humidity of 85%. These findings suggest that the films proceed in a similar and efficient manner, with significant degradation taking place over a short timeframe [51].

The algal polysaccharides used for film forming are biodegradable; these include galactans, alginates, and ulvan, and have shown tremendous potential in the development

of novel packaging materials with improved barrier, mechanical, antioxidant, and antimicrobial properties [10,18]. In a recent study [31], metalloanthocyanin-inspired biodegradable packaging films were developed by incorporating purple cauliflower extracted anthocyanins into alginate/carboxymethyl chitosan hybrid polymer matrices. The addition of fucoidan further enhanced the mechanical and antibacterial activity of the films. These complexation processes also resulted in improved storage stability and antioxidant capability while reducing the release rate of anthocyanins. The development of edible films and coatings has seen substantial growth in recent years and is expected to significantly impact the quality of food products in the future. Additionally, research into polysaccharide-based films with ionic inclusion liquids (ILs) and deep eutectic solvents (DESs) as potential replacements for conventional solvents/plasticizers has shown promising results [10,18]. Blended films consisting of sodium carboxymethylcellulose (CMC), chitosan (CS), sodium alginate (SA), glycerol, and $CaCl_2$ as plasticizer/crosslinker enriched with monobasic ammonium phosphate have also demonstrated increased water resistance and thermal stability while enhancing biodegradability [62].

4. Conclusions

Lithraea molleoides fruit gum (LMFG) is a valuable product obtained from the total hydrolysis of the fruit. The hydrolysis process involves three methods: thermal (LMFGT), alkaline (LMFGB), and acid (LMFGA). The yield for the LMFGB flour was 33.88%, 15.43% for the LMFGA, and 11.11% for the LMFGT. This means that alkaline hydrolysis is more efficient in extracting polysaccharide, while thermal hydrolysis is less efficient. In reference [43], where the molecular weight for LMFGB is 85,000 g/mol, followed in ascending order by LMFGT with a value of 195,000 g/mol and ending with LMFGA with 589,000 g/mol, these molecular weight values largely justify the behavior of the resulting films. The resulting hydrolysates are then combined with pectins in a 1:2 ratio to form films. In this study, the focus was on utilizing the hydrolysates of *Lithraea molleoides* gums for film applications, with an evaluation of their structural and physicochemical characteristics. The films produced exhibited excellent mechanical properties that are comparable to pectin film (Pec2.5) and low water vapor permeability. Thermal stability was up to 200 °C with T_g between 40 and 50 °C and T_m from 132 to 143 °C, which indicates an excellent material that can be extruded and is also thermally resistant. The film blends demonstrated showed biodegradability within ten days, but pectin film were seven days, which may be due to the presence of antioxidants providing protection against soil microorganisms [63].

The packaging capacity was strengthened since it has a certain protection due to its antioxidant capacity. The suggested application for this type of film is for storing dry products, such as flour, sugar, etc.

Author Contributions: Conceptualization, F.B. and M.M.; methodology, F.B.; validation, M.F.G. and G.M.; formal analysis, F.B. and G.M.; investigation, M.F.G.; resources, M.M.; writing—original draft preparation, F.B. and M.M.; writing—review and editing, F.B., M.F.G. and M.M. All authors have read and agreed to the published version of the manuscript.

Funding: PICT-2020-SERIEA-00895 (RAICES). Title: "Obtención de Polisacáridos a partir de Vegetales y Microorganismos de la Región del Semiárido de San Luis. Aplicaciones: Alimentarias, Geles y Bioempaque", 2. PROICO 2-3423, UNSL: "Bioprospección de Recursos Autóctonos Vegetales y Microbianos de la Provincia de San Luis con Potencial Uso Biotecnológico", and 3. PIP 2021/2023, IF-2021-85081432-APN-DCP#CONICET, "Valorización biotecnológica de efluentes de destilería para la obtención de productos microbianos".

Data Availability Statement: The original contributions presented in the study are included in the article; further inquiries can be directed to the corresponding authors.

Acknowledgments: The authors thank the following institutions in Argentina: Instituto de Física Aplicada (INFAP-UNSL-CONICET) and Laboratorio de Investigación y Servicios de Química Física (LISeQF-UNSL). The authors also thank Javier Rigau from the Instituto de Investigación en Tecnología Química (INTEQUI-UNSL-CONICET) for their determinations of the FTIR, TGA, and DSC, and Ariel Ochoa from the Laboratorio de Membranas y Biomateriales del INFAP-CONICET-UNSL for their contributions to the mechanical test and water vapor permeability results.

Conflicts of Interest: The authors declare no conflicts of interest.

References

1. Kadac-Czapska, K.; Knez, E.; Gierszewska, M.; Olewnik-Kruszkowska, E.; Grembecka, M. Microplastics derived from food packaging waste—Their origin and health risks. *Materials* **2023**, *16*, 674.
2. Ferreira, M.S.; Linhares, R.; Martelli, M. Films and coatings from agro-industrial residues. In *Edible Films and Coatings*; CRC Press: London, UK, 2016; Chapter 11, pp. 211–232.
3. Nussinovitch, A. Biopolymer films and composite coatings. In *Modern Biopolymer Science*; Academic Press: London, UK, 2009; pp. 295–326.
4. da Silva, M.A.; Bierhalz, A.C.K. Biopolymer Films and Composite Coatings: Applications. In *Handbook of Biopolymers*; Springer Nature: Singapore, 2023; pp. 1229–1261
5. Lopez, O.V.; Garcia, M.A.; Zaritzky, N.E. Novel sources of edible films and coatings. *Stewart Postharvest Rev.* **2010**, *6*, 1–8.
6. Beyza, H.; Fatma, K.; Hecer, C. Edible films and coatings: A good idea from past to future technology. *J. Food Technol*. **2018**, *5*, 28–33.
7. Campos, C.A.; Gerschenson, L.N.; Flores, S.K. Development of edible films and coatings with antimicrobial activity. *Food Bioprocess Technol.* **2011**, *4*, 849–875.
8. Dyshlyuk, L.; Babich, O.; Belova, D.; Prosekov, A. Comparative analysis of physical and chemical properties of biodegradable edible films of various compositions. *J. Food Process Eng.* **2017**, *40*, e12331.
9. Subroto, E.; Indiarto, R.; Pangawikan, A.D.; Prakoso, F. Production and Characteristics of Composite Edible Films Based on Polysaccharides and Proteins. *Int. J. Emerg. Trends Eng. Res.* **2021**, *9*, 42–48.
10. Han, J.H. Edible films and coatings: A review. In *Innovations in Food Packaging*; Academic Press: San Diego, CA, USA, 2014; Chapter 9, pp. 213–255.
11. Šuput, D.Z.; Lazić, V.L.; Popović, S.Z.; Hromiš, N.M. Edible films and coatings: Sources, properties and application. *Food Feed. Res.* **2015**, *42*, 11–22.
12. Liyanapathiranage, A.; Dassanayake, R.S.; Gamage, A.; Karri, R.R.; Manamperi, A.; Evon, P.; Jayakodi, Y.; Madhujith, T.; Merah, O. Recent developments in edible films and coatings for fruits and vegetables. *Coatings* **2023**, *13*, 1177.
13. Drevet, R.; Benhayoune, H. Advanced Biomaterials and Coatings. *Coatings* **2022**, *12*, 965.
14. Marangoni Júnior, L.; Coltro, L.; Dantas, F.B.H.; Vieira, R.P. Research on food packaging and storage. *Coatings* **2022**, *12*, 1714.
15. Dhanapal, A.; Sasikala, P.; Rajamani, L.; Kavitha, V.; Yazhini, G.; Banu, S. Edible films from polysaccharides. *Food Sci. Qual. Manag.* **2012**, *3*, 9–17.
16. Kocira, A.; Kozłowicz, K.; Panasiewicz, K.; Staniak, M.; Szpunar-Krok, E.; Hortyńska, P. Polysaccharides as edible films and coatings: Characteristics and influence on fruit and vegetable quality—A review. *Agronomy* **2021**, *11*, 813.
17. Nieto, M.B. Structure and function of polysaccharide gum-based edible films and coatings. In *Edible Films and Coatings for Food Applications*; Springer-Nature: Berlin, Germany, 2009; Chapter 2, pp. 57–112.
18. Galus, S.; Arik Kibar, E.A.; Gniewosz, M.; Kraśniewska, K. Novel materials in the preparation of edible films and coatings—A review. *Coatings* **2020**, *10*, 674.
19. Avramescu, S.M.; Butean, C.; Popa, C.V.; Ortan, A.; Moraru, I.; Temocico, G. Edible and functionalized films/coatings—Performances and perspectives. *Coatings* **2020**, *10*, 687.
20. Falguera, V.; Quintero, J.P.; Jiménez, A.; Muñoz, J.A.; Ibarz, A. Edible films and coatings: Structures, active functions and trends in their use. *Trends Food Sci. Technol.* **2011**, *22*, 292–303.
21. Brasselet, C.; Pierre, G.; Dubessay, P.; Dols-Lafargue, M.; Coulon, J.; Maupeu, J.; Vallet-Courbin, A.; de Baynast, H.; Doco, T.; Michaud, P.; et al. Modification of chitosan for the generation of functional derivatives. *Appl. Sci.* **2019**, *9*, 1321.
22. Roman, M.; Nechita, P.; Vasile, M.A.; Cantaragiu Ceoromila, A.M. Barrier and Antimicrobial Properties of Coatings Based on Xylan Derivatives and Chitosan for Food Packaging Papers. *Coatings* **2023**, *13*, 1761.
23. Pinto, J.P.; D'souza, O.J.; Hiremani, V.D.; Dalbanjan, N.P.; Kumar, S.P.; Narasagoudr, S.S.; Masti, S.P.; Chougale, R.B. Functional properties of taro starch reinforced polysaccharide based films for active packaging. *Food Biosci.* **2023**, *56*, 103340.
24. Chang, S.; Zou, X.; Zhu, B.; You, L.; Zhao, Z.; Hileuskaya, K. The characteristics of polysaccharide from *Gracilaria chouae* and its application in food packaging with carboxymethyl cellulose and lysozyme. *Food Hydrocoll.* **2023**, *135*, 108109.
25. Long, J.; Zhang, W.; Zhao, M.; Ruan, C.Q. The reduce of water vapor permeability of polysaccharide-based films in food packaging: A comprehensive review. *Carbohydr. Polym.* **2023**, *321*, 121267.
26. Tang, H.; Han, Z.; Zhao, C.; Jiang, Q.; Tang, Y.; Li, Y.; Cheng, Z. Preparation and characterization of Aloe vera polysaccharide-based packaging film and its application in blueberry preservation. *Prog. Org. Coat.* **2023**, *177*, 107445.

27. Carneiro-da-Cunha, M.G.; Cerqueira, M.A.; Souza, B.W.; Souza, M.P.; Teixeira, J.A.; Vicente, A.A. Physical properties of edible coatings and films made with a polysaccharide from *Anacardium occidentale* L. *J. Food Eng.* **2009**, *95*, 379–385.
28. Salama, A.; El-Sakhawy, M. Polysaccharides/propolis composite as promising materials with biomedical and packaging applications: A review. *Biomass Convers. Biorefinery* **2024**, *14*, 4555–4565.
29. Gharibzahedi, S.M.T.; Ahmadigol, A.; Khubber, S.; Altintas, Z. Bionanocomposite films with plasticized WPI-jujube polysaccharide/starch nanocrystal blends for packaging fresh-cut carrots. *Food Packag. Shelf Life* **2023**, *36*, 101042.
30. Huang, J.; Wu, W.; Niu, B.; Fang, X.; Chen, H.; Wang, Y.; Gao, H. Characterization of *Zizania latifolia* polysaccharide-corn starch composite films and their application in the postharvest preservation of strawberries. *LWT* **2023**, *173*, 114332.
31. Song, X.; Wang, X.; Zhang, H.; Zhang, D.; Li, Z.; Yu, J. Characterization of polysaccharide-based antibacterial films properties of loaded with Nisin and preservation of fresh-cut watermelon. *Food Sci. Technol.* **2023**, *43*, e127522.
32. Zheng, M.; Zhu, Y.; Zhuang, Y.; Tan, K.B.; Chen, J. Effects of grape seed extract on the properties of pullulan polysaccharide/xanthan gum active films for apple preservation. *Int. J. Biol. Macromol.* **2023**, *241*, 124617.
33. Jafarian, M.; Taghinia, P.; Sedaghati, S. Development and characterization of a new active and intelligent packaging system based on soluble soybean polysaccharide-*Malva sylvestris* extract. *J. Food Sci. Technol.* **2023**, *60*, 1944–1951.
34. Yu, T.; Wu, D.; Liang, B.; Wang, J.; Shang, X.; Wu, Q. Preparation, characterization of Auricularia auricula polysaccharide-based films and application in meat preservation. *Int. J. Biol. Macromol.* **2023**, *244*, 125242.
35. Janik, W.; Jakubski, Ł.; Kudła, S.; Dudek, G. Modified polysaccharides for food packaging applications: A review. *Int. J. Biol. Macromol.* **2023**, *258*, 128916.
36. Akhtar, H.M.S.; Ahmed, S.; Olewnik-Kruszkowska, E.; Gierszewska, M.; Brzezinska, M.S.; Dembińska, K.; Kalwasińska, A. Carboxymethyl cellulose based films enriched with polysaccharides from mulberry leaves (*Morus alba* L.) as new biodegradable packaging material. *Int. J. Biol. Macromol.* **2023**, *253*, 127633.
37. Sarkar, S.; Manna, S.; Das, S.; De, S.; Paul, P.; Dua, T.K.; Sahu, R.; Nandi, G. Current Status of Marine Animal Derived Polysaccharides in Sustainable Food Packaging. *ACS Food Sci. Technol.* **2023**, *3*, 1877–1889.
38. Liu, J.; Dong, Y.; Zheng, X.; Pei, Y.; Tang, K. Citric acid crosslinked soluble soybean polysaccharide films for active food packaging applications. *Food Chem.* **2024**, *438*, 138009.
39. Chi, K.; He, J.; Lin, W.S.; Bokhari, S.M.; Catchmark, J.M. Electrostatically complexed natural polysaccharides as aqueous barrier coatings for sustainable and recyclable fiber-based packaging. *ACS Appl. Mater. Interfaces* **2023**, *15*, 12248–12260.
40. Kaya, E.C.; Yucel, U. Advances in cellulose-based packaging films for food products. In *Cellulose—Fundamentals and Conversion into Biofuel and Useful Chemicals*; Intech Open: London, UK, 2023; pp. 1–21.
41. Dong, Y.; Li, Y.; Ma, Z.; Rao, Z.; Zheng, X.; Tang, K.; Liu, J. Effect of polyol plasticizers on properties and microstructure of soluble soybean polysaccharide edible films. *Food Packag. Shelf Life* **2023**, *35*, 101023.
42. Garro, M.F.; Salinas Ibáñez, A.G.; Vega, A.E.; Arismendi Sosa, A.C.; Pelzer, L.; Saad, J.R.; Maria, A.O. Gastroprotective effects and antimicrobial activity of *Lithraea molleoides* and isolated compounds against Helicobacter pylori. *J. Ethnopharmacol.* **2015**, *176*, 469–474.
43. Becerra, F.; Garro, M.F.; Masuelli, M. Influence of the Type of Hydrolysis on the Intrinsic Viscosity of *Lithraea molleoides* Fruit Gum. *J. Mater. Polym. Sci.* **2023**, *3*, 1–6.
44. Rulli, M.M.; Villegas, L.B.; Barcia, C.S.; Colin, V.L. Bioconversion of sugarcane vinasse into fungal biomass protein and its potential use in fish farming. *J. Environ. Chem. Eng.* **2021**, *9*, 106136.
45. Deng, C.; Hu, Z.; Fu, H.; Hu, M.; Xu, X.; Chen, J. Chemical analysis and antioxidant activity in vitro of β-D-glucan isolated from *Dictyophora indusiate*. *Int. J. Biol. Macromol.* **2012**, *51*, 70–75.
46. Kaur, R.; Arora, S.; Singh, B. Antioxidant activity of the phenol rich fractions of leaves of *Chukrasia tabularis* A. Juss. *Bioresour. Technol.* **2008**, *99*, 7692–7698.
47. Ainsworth, E.A.; Gillespie, K.M. Estimation of total phenolic content and other oxidation substrates in plant tissues using Folin–Ciocalteu reagent. *Nat. Protoc.* **2007**, *2*, 875–877.
48. Zanon, M.; Masuelli, M. Purification and characterization of alcayota gum. *Biopolym. Res.* **2018**, *2*, 105.
49. Al Sagheer, F.A.; Al-Sughayer, M.A.; Muslim, S.; Elsabee, M.Z. Extraction and characterization of chitin and chitosan from marine sources in Arabian Gulf. *Carbohydr. Polym.* **2009**, *77*, 410–419.
50. Barbosa, H.F.; Francisco, D.S.; Ferreira, A.P.; Cavalheiro, É.T. A new look towards the thermal decomposition of chitins and chitosans with different degrees of deacetylation by coupled TG-FTIR. *Carbohydr. Polym.* **2019**, *225*, 115232.
51. Zanon, M.; Masuelli, M.A. Alcayota gum films: Experimental reviews. *J. Mater. Sci. Chem. Eng.* **2018**, *6*, 11–58.
52. Lazo, L.; Melo, G.M.; Auad, M.L.; Filippa, M.; Masuelli, M.A. Synthesis and characterization of Chañar gum films. *Colloids Interfaces* **2022**, *6*, 10.
53. Illanes, C.O.; Takara, E.A.; Masuelli, M.A.; Ochoa, N.A. pH-responsive gum tragacanth hydrogels for high methylene blue adsorption. *J. Chem. Technol. Biotechnol.* **2024**, *99*, 31–39.
54. Masuelli, M.A.; Lazo, L.; Becerra, F.; Torres, F.; Illanes, C.O.; Takara, A.; Auad, M.L.; Bercea, M. Physical and Chemical Properties of *Pachycymbiola brasiliana* Eggshells—From Application to Separative Processes. *Processes* **2024**, *12*, 814.
55. Zapata-Luna, R.L.; Davidov-Pardo, G.; Pacheco, N.; Ayora-Talavera, T.; Espinosa-Andrews, H.; García-Márquez, E.; Cuevas-Bernardino, J.C. Structural and physicochemical properties of bio-chemical chitosan and its performing in an active film with quercetin and *Phaseolus polyanthus* starch. *Rev. Mex. Ing. Química* **2023**, *22*, 1–11.

56. Acosta-Ferreira, S.; Castillo, O.S.; Madera-Santana, J.T.; Mendoza-García, D.A.; Núñez-Colín, C.A.; Grijalva-Verdugo, C.; Villa-Lerma, A.G.; Morales-Vargas, A.T.; Rodríguez-Núñez, J.R. Production and physicochemical characterization of chitosan for the harvesting of wild microalgae consortia. *Biotechnol. Rep.* **2020**, *28*, e00554.
57. Chel-Guerrero, L.; Betancur-Ancona, D.; Aguilar-Vega, M.; Rodríguez-Canto, W. Films properties of QPM corn starch with *Delonix regia* seed galactomannan as an edible coating material. *Int. J. Biol. Macromol.* **2024**, *255*, 128408.
58. Leite, K.; Nascimento, J.; Neto, J.H.L.; Gomes, K. Influence of citric acid on the properties of galactomanan bioplastics from *Prosopis juliflora* (Sw.) DC.: Influência do ácido cítrico nas propriedades dos bioplásticos de galactomanana de *Prosopis juliflora* (sw.) DC. *Concilium* **2024**, *24*.
59. Meng, F.; Zhang, Y.; Xiong, Z.; Wang, G.; Li, F.; Zhang, L. Mechanical, hydrophobic and thermal properties of an organic-inorganic hybrid carrageenan-polyvinyl alcohol composite film. *Compos. Part B Eng.* **2018**, *143*, 1–8.
60. Ruano, P.; Lazo Delgado, L.; Picco, S.; Villegas, L.; Tonelli, F.; Aguilera Merlo, M.E.; Rigau, J.; Diaz, D.; Masuelli, M. Extraction and Characterization of Pectins from Peels of Criolla Oranges (*Citrus sinensis*): Experimental Reviews. In *Pectins—Extraction, Purification, Characterization and Applications*; Masuelli, M., Ed.; Intech Publishers: London, UK, 2020; Chapter 1.
61. Lin, X.; Chen, S.; Wang, R.; Li, C.; Wang, L. Fabrication, characterization and biological properties of pectin and/or chitosan-based films incorporated with noni (*Morinda citrifolia*) fruit extract. *Food Hydrocoll.* **2023**, *134*, 108025.
62. Ciaramitaro, V.; Piacenza, E.; Paliaga, S.; Cavallaro, G.; Badalucco, L.; Laudicina, V.A.; Chillura Martino, D.F. Exploring the Feasibility of Polysaccharide-Based Mulch Films with Controlled Ammonium and Phosphate Ions Release for Sustainable Agriculture. *Polymers* **2024**, *16*, 2298.
63. Li, H.; Li, Z.; Wang, P.; Liu, Z.; An, L.; Zhang, X.; Xie, Z.; Li, X.; Gao, W. Evaluation of citrus pectin extraction methods: Synergistic enhancement of pectin's antioxidant capacity and gel properties through combined use of organic acids, ultrasonication, and microwaves. *Int. J. Biol. Macromol.* **2024**, *266*, 131164.